

# CHARACTERIZATION OF THE PEDIATRIC CHEST AND ABDOMEN USING THREE POST-MORTEM HUMAN SUBJECTS

**Richard Kent, Francisco J. Lopez-Valdes, John Lamp, Sabrina Lau, Daniel Parent, Jason Kerrigan, David Lessley, Robert Salzar**

Center for Applied Biomechanics, University of Virginia

United States

Paper Number 11-0394

## ABSTRACT

This paper reports a series of experiments on 6, 7, and 15 year-old pediatric post-mortem human subjects (PMHS) undertaken to guide the scaling of existing adult thoracic response data for application to the child and to assess the validity of a juvenile porcine abdominal model. The pediatric PMHS exhibited abdominal response similar to the swine, including the degree of rate sensitivity. The thoraces of the PMHS were as stiff as, or slightly more stiff than, published adult corridors. An assessment of age-related changes in thoracic stiffness supports our earlier suggestion (2009) that the effective stiffness of the chest increases through the fourth decade of life and then decreases, resulting in stiffness values similar for children and elderly adults.

## INTRODUCTION

Motor vehicle crashes are the leading cause of death and injury for children in the United States and head injuries are of principal concern for children involved in crashes. Regardless of the age group or crash direction, injuries to the brain and skull are the most common serious injuries sustained by children in crashes (Arbogast et al. 2002, 2004 and 2005, Durbin et al. 2003, Orzechowski et al. 2003) and are responsible for one-third of all pediatric injury deaths (Adekoya et al. 2002, Thompson et al. 2003). The abdomen is the second most commonly injured body region in young children using vehicle seat belts, and can be associated with significant health care costs and extended hospitalization (Bergqvist et al. 1985, Tso et al. 1993, Trosseille et al. 1997, Durbin et al. 2001).

The trajectory and attitude of the head during an impact are dictated by, among other factors, the interaction of the restraint system with the trunk.

Any thoracic model must represent this interaction in a biofidelic manner to ensure that restraint designs protect humans as intended. Despite the importance of this interaction and of abdominal loading as an injury mechanism in children, benchmarking data for pediatric models of the trunk are lacking.

The biomechanics of the pediatric abdomen have recently been described in detail using a juvenile swine model (Kent et al. 2006, 2008). The model was benchmarked against quasistatic human volunteer experiments and against the distribution of injuries sustained by children in the field, but was not benchmarked against pediatric force-deformation behavior in the high-rate, high-deformation loading environment relevant to crash conditions. Ouyang et al. (2006) reported thoracic blunt hub impact tests of nine PMHS aged 2 – 12 years, but the use of these experiments to elucidate thoracic response to belt loading is uncertain (see Kent et al. 2004). In 2009, Kent et al. reported a series of dynamic thoracoabdominal belt loading experiments using a 7-year-old PMHS, but acknowledged that the analysis was limited by use of a single subject.

Hence, there is currently a need for pediatric thoracoabdominal mechanics data in contemporary loading situations (non-impact harness loading). The objective of this study is to expand the dataset reported by Kent et al. 2009 with the inclusion of two additional pediatric PMHS. This paper reports a composite dataset of all three pediatric PMHS.

## MATERIALS AND METHODS

### Specimens

Three pediatric PMHS (Table 1) were obtained and tested in accordance with the ethical guidelines established by the Human Usage Review Panel of the

National Highway Traffic Safety Administration, and with the approval of the Office of the Vice President for Research and an independent Oversight Committee at the University of Virginia, and Institutional Review Boards at Duke University and The Children’s Hospital of Philadelphia.

**Table 1.**  
**Specimen Descriptions**

Specimen ID		DukeF (470F)	484F	485M
Gender		F	F	M
Age at Death (years)		7	6	15
Whole-body mass (kg)		26.8	24.0	50.0
Torso breadth (mm)	4th Rib	273	217	271
	8th Rib	270	202	240
	Umbilicus	278	217	239
Torso depth (mm)	4th Rib	155	142	131
	8th Rib	172	140	142
	Umbilicus	161	122	106
Torso circumference (mm)	4th Rib	695	602	718
	8th Rib	698	593	646
	Umbilicus	701	590	595
Anatomical Lengths (along axis of body) (mm)				
Stature		1194	1280	1700
Sternal notch to xiphoid		114	130	172
Xiphoid to umbilicus		131	159	203
Vertex to pubic symphysis (seated height)		625	640	840

See Kent et al. (2009) for a detailed description of the 7 year-old female subject. The cause of death of the 6 year-old female was germ cell malignancy, but no acute gonadal tumors were found either in pre-test CT scans or during a post-test thoracoabdominal necropsy. Prior to the time of death the subject was on a ventilator and pre-test CT scans revealed an L5 vertebra plana, several cystic lung lesions, which is consistent with ventilator pneumonia, as well as visceral gas, evidence of postmortem necrosis. The subject was approximately 95th percentile in stature for a 6 year-old female, and between the 75th and 90th percentile for mass (Ogden et al. 2002). The cause of death of the 15 year-old male was malignant thalamic glioblastoma. A review of CT scans revealed mild dextroscoliosis of the thoracic spine, moderate bilateral pneumothoraces, and scattered gas, evidence of post mortem necrosis. The 15-year-old subject was approximately 50th percentile in stature and 25th percentile in mass, and was severely emaciated. The level of emaciation was deemed

sufficient to render that subject’s abdominal response meaningless (the anterior aspect of the lumbar spine was less than 5 mm posterior of the anterior abdominal wall). Upon receipt, the PMHS were stored in a freezer (-15°C) until they were removed and thawed at room temperature for at least 36 hours prior to testing. Computed tomography (CT) scans verified the absence of preexisting fractures or other bone pathology in all specimens, with the exception of sagittal asymmetry due to moderate scoliosis in the 7 year-old female.

## Test Hardware and Methods

A hydraulic master-slave cylinder arrangement connecting a high-speed material testing machine to a table-top test rig was employed in this test series. The test rig is similar to that used previously by Kent et al. (2004) to allow for diagonal and distributed belt loading with defined anchor points. The test rig consisted of a frame made of steel tubing that supported slave cylinders (Figure 1, see additional images in Kent et al. 2009). In diagonal belt tests of the thorax, the cylinders drove a carriage, guided by linear bearings, up and down. The carriage was connected to the 5-cm-wide diagonal belt via steel cables that passed over pulleys. In the abdominal and distributed loading tests, the belt was attached directly to the slave cylinder pistons via steel cables that passed through channels cut in the center of the specimen-supporting hardware.

For the abdominal tests, a 5-cm-wide belt (similar to that used in Kent et al. 2006, 2008) was used. For the distributed belt tests, a 16.8-cm-wide belt was used on the 6 and 7 year-olds and a 20.3-cm-wide belt was used on the 15 year-old (the same distributed belt used on the adults reported by Kent et al. 2004). The distributed belt geometry was determined by scaling the belt geometry from the adult testing (Kent et al. 2004) using an average of scale factors relating the adult thoracic anthropometry to that of the pediatric PMHS. Polyethylene fiber-reinforced composite (Spectra®, E = 97 GPa) material was used for all belts rather than actual seatbelt webbing (which would stretch nominally 2%-4% in these tests) to isolate the thoracic response from a combined effect that includes belt stretch. The top of the test rig consisted of an aluminum plate attached to a load cell used to measure posterior reaction forces and moments. Plywood sheets were used to adjust the specimen’s height on the table to achieve realistic belt angles off of the shoulder and pelvis.

The diagonal belt passed over the left shoulder and crossed the anterior thorax approximately 30° from

the mid-sagittal plane. The centerline of the belt crossed the left clavicle approximately 60 mm from the sagittal plane, and exited the body at approximately the 10th rib laterally. For the distributed belt loading, the belt was centered over the xiphoid. Lower abdominal loading was conducted with the belt centered on the umbilicus (for the 7 year-old) and with the belt centered 29 mm

superior of the umbilicus (for the 6 year-old). Upper abdominal loading on the 7 year-old was performed with the belt centered 7 cm superior to the umbilicus (6.1 cm inferior to the xiphoid process). The upper abdominal loading location on the 6-year old was with the belt centered 7.6 cm superior of the umbilicus (6.4 cm inferior to xiphoid process).

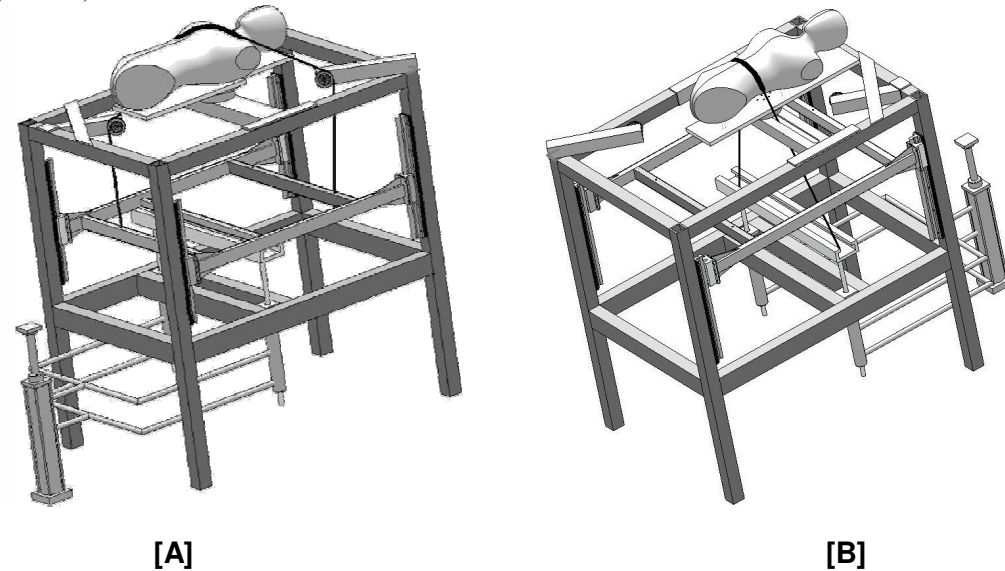


**Figure 1. Table top test rig schematic in diagonal belt configuration ([A]) and abdominal configuration ([B]).**

The table-top was instrumented with a six-axis load cell under the posterior support plate and tension load cells attached to the cable-belt system. Load cell data were sampled at 10 kHz with a DEWE-2600 (Dewetron Inc., Wakefield, RI) data acquisition system and hardware (anti-aliasing) filtered. The data were later processed with a low-pass 100 Hz 8-pole Butterworth filter. Kinematic data were sampled at 1000 Hz using an eight-camera Vicon MX™ three-dimensional (3D) motion capture system that tracked the motion of retroreflective spherical targets through a calibrated 3D space. The input displacement to the subject for each test condition was measured using targets secured to the belt. For all belt tests, displacement was measured using a single target secured at the intersection of the belt center line and the mid-sagittal plane. Displacements for all tests were calculated with respect to a spine-based SAE occupant coordinate system, in which the positive Z-axis was directed inferiorly along the spine and the positive X-axis was directed perpendicularly to the spine and toward the sternum, lying in the midsagittal plane. The X-axis displacement defined “chest displacement” for thoracic characterization and “penetration” for abdominal characterization. For ease of interpretation, all of the results present the absolute value of the magnitude of the chest

displacement, the abdominal penetration, and the posterior reaction force (i.e., positive sign), though the direction of the displacement was toward the spine.

After thawing the specimen, a tracheal tube was inserted to facilitate lung inflation. Prior to each test, a syringe was used to inflate the lungs with 300 mL of air via the tube, and then remove the same amount of air. A series of five inflation cycles was performed before a final inflation was performed. The air was free to flow in and out of the tube during the tests.

A series of 24 displacement-controlled tests was performed to measure the thorax/abdomen response under the four loading conditions (Table 2). A minimum of 10 minutes separated tests. Before each test, a nominal pretension load of 8 N was applied to each end of the belt. After all testing, the skin and superficial tissue of the torso were removed to assist in the process of identifying injuries. After palpating the rib cage for fractures, the specimens were CT scanned at high resolution (0.59 mm in-plane and 0.63 mm slice thickness), and a radiologist read the scans to assist in identification of any rib fractures or other trauma.

## RESULTS

In general, consideration of two additional PMHS did not change the broad conclusions drawn by Kent et al. (2009) following the tests on the 7 year-old. The 6 year-old exhibited both thoracic and abdominal response similar to the 7 year-old, while the 15 year-old exhibited slightly stiffer thoracic response.

### Abdominal Loading

Quasistatic and dynamic tests on the lower abdomen and dynamic tests on the upper abdomen were successfully performed on both female subjects. The responses were remarkably similar for the two subjects. Both subjects exhibited stiffer behavior in the dynamic test, and in the lower abdomen compared to the upper (Figure 2). The lower abdomen generated approximately 4-5 kN at 35 mm

of dynamic penetration, while the upper generated only approximately 2.5 kN. The lower abdomen generated approximately 1 kN at 28 mm of quasistatic penetration.

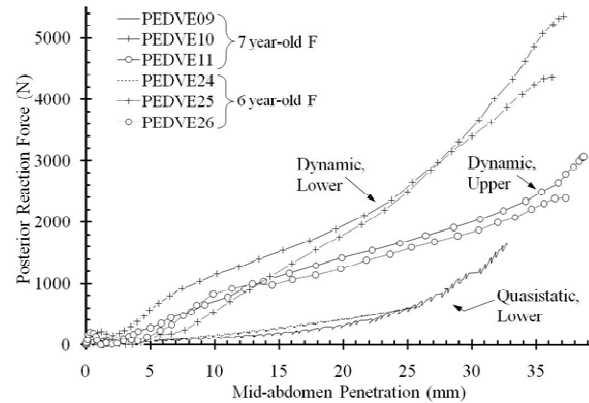


**Figure 2. Biomechanical response to transverse belt loading on the abdomen (7 year-old and 6-year-old females).**

**Table 2. Test Matrix**

DAQ Index	Subject	Region	Loading Type	Description	Peak Input Displacement	Peak Posterior Reaction Force
PEDVE09	DukeF	L. Abdomen	Transverse belt	Quasistatic	32.6 mm	1,608 N
PEDVE10	DukeF	L. Abdomen	Transverse belt	Dynamic <sup>1</sup>	37.1 mm	5,352 N
PEDVE11	DukeF	U. Abdomen	Transverse belt	Dynamic	38.6 mm	3,051 N
PEDVE12	DukeF	Chest	Distributed belt	1-Hz	27.5 mm	2,826 N
PEDVE13	DukeF	Chest	Distributed belt	Dynamic	31.0 mm	6,620 N
PEDVE14	DukeF	Chest	Distributed belt	0.5 Hz, 4 Hz	25.8 mm	3,417 N
PEDVE15	DukeF	Chest	Diagonal belt	1-Hz	33.0 mm	1,240 N
PEDVE16	DukeF	Chest	Diagonal belt	Dynamic	34.9 mm	3,513 N
PEDVE17	DukeF	Chest	Diagonal belt	0.5 Hz, 4 Hz	32.0 mm	1,248 N
PEDVE18	DukeF	Chest	Diagonal belt	Dynamic	37.1 mm	4,378 N
PEDVE19	DukeF	Chest	Diagonal belt	Dynamic	52.0 mm	5,941 N
PEDVE24	484F	L. Abdomen	Transverse belt	Quasistatic	25.7 mm	607 N
PEDVE25	484F	L. Abdomen	Transverse belt	Dynamic <sup>1</sup>	36.2 mm	4,363 N
PEDVE26	484F	U. Abdomen	Transverse belt	Dynamic	37.3 mm	2,389 N
PEDVE29	484F	Chest	Distributed belt	Dynamic	34.3 mm	4,224 N
PEDVE30	484F	Chest	Distributed belt	Dynamic	39.2 mm	6,968 N
PEDVE31	484F	Chest	Diagonal belt	1-Hz	30.6 mm	934 N
PEDVE32	484F	Chest	Diagonal belt	Dynamic	41.9 mm	2,943 N
PEDVE33	484F	Chest	Diagonal belt	Dynamic	42.0 mm	3,155 N
PEDVE34	484F	Chest	Diagonal belt	Dynamic	54.6 mm	5,195 N
PEDVE40	485M	Chest	Distributed belt	1-Hz	21.7 mm	1,574 N
PEDVE41	485M	Chest	Distributed belt	Dynamic	27.3 mm	4,533 N
PEDVE42	485M	Chest	Diagonal belt	1-Hz	23.1 mm	1,359 N
PEDVE43	485M	Chest	Diagonal belt	Dynamic	32.5 mm	3,977 N

See Kent et al. (2009) for detailed discussion of rate. All abdomen tests fall in "Rate Bin 1" from Kent et al. (2006).

### Thoracic loading from a diagonal belt

Quasistatic and dynamic (approximately 1.5 m/s input belt displacement rate) tests with diagonal belt loading were successfully performed on all three

subjects. As with the abdominal loading, the two younger females exhibited remarkably similar response. The 15 year-old male was slightly stiffer at both rates (Figure 3).

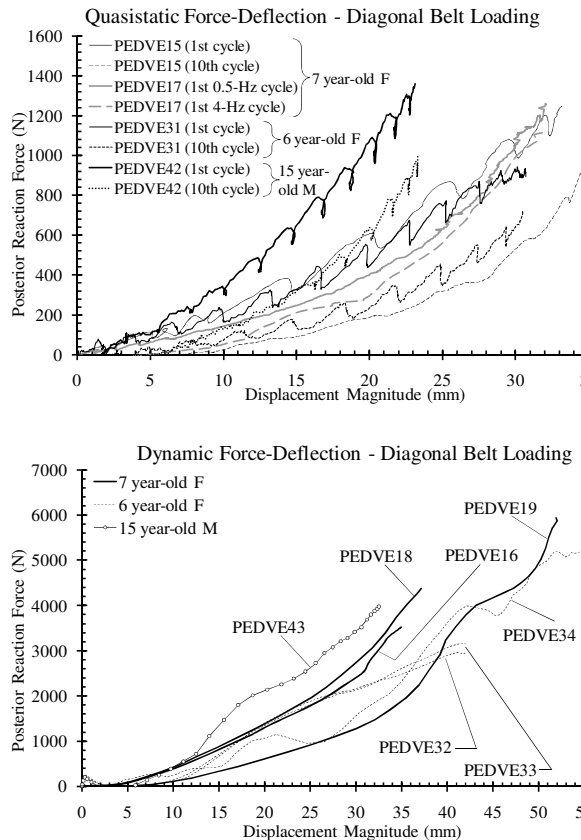


**Figure 3. Biomechanical response to diagonal belt loading on the thorax (7 year-old and 6-year-old females, 15 year-old male) at quasistatic (top) and dynamic (bottom) rates.**

### Thoracic loading from a distributed belt

Quasistatic tests with distributed loading were successfully performed on the 7 year-old female and on the 15 year-old male. Dynamic (approximately 1.5 m/s input displacement rate) tests with distributed loading were successfully performed on all three subjects. The 7 year-old and the 15 year-old exhibited similar quasistatic behavior, while the 7 year-old had the stiffest dynamic response (Figure 4).

### Trauma generated

Two rib fractures were identified during the post-test autopsy of the 6 year-old: one fracture on each of the 2<sup>nd</sup> and 3<sup>rd</sup> ribs on the left aspect. Since the diagonal belt passed over the left shoulder, these fractures are both in the region of concentrated diagonal belt loading. The 7 year-old sustained a total of 13 rib fractures. On the left side, ribs 2-6 were fractured approximately 1 cm from the costochondral junction. On the right side ribs 4-7 were fractured

approximately 1 cm from the costochondral junction, and ribs 3-6 sustained lateral fractures. Comparison with CT scans taken before any testing was performed confirms that the fractures were generated during the test series. The pattern suggests that the fractures were generated with diagonal belt loading and comparison of the responses measured in tests PEDVE16, PEDVE18, and PEDVE19 suggests that the structural stability of the rib cage was not compromised prior to the performance of test PEDVE18, but was afterwards. No rib fractures were observed on the 15 year-old subject. None of the subjects sustained any gross abdominal injury.

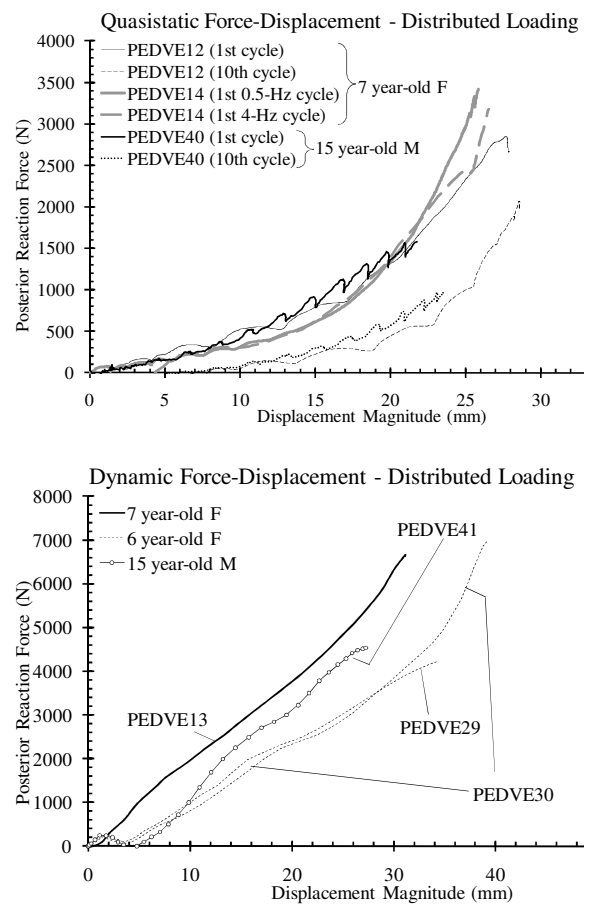
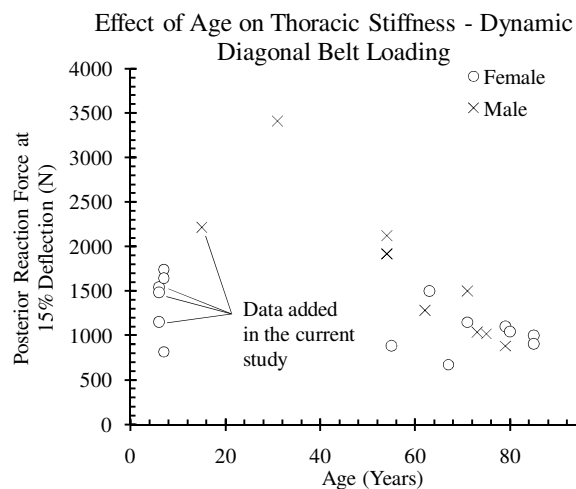


**Figure 4. Biomechanical response to distributed loading on the thorax (7 year-old and 6-year-old females, 15 year-old male) at quasistatic (top) and dynamic (bottom) rates.**

### DISCUSSION AND CONCLUSIONS

The key contribution of this study is the expansion of the analysis originally published by Kent et al. (2009) with the addition of two pediatric subjects. Now,

based on a total of 3 pediatric PMHS tested utilizing an experimental protocol and scaled test apparatus used to characterize 15 adults PMHS (Kent et al. 2004, Salzar et al. 2009), the two main conclusions drawn in that earlier study can be re-stated with more confidence. First, the abdominal response of the juvenile swine seems to be a reasonable benchmark for the Hybrid III 6 year-old abdominal insert. The 6 year-old subject exhibited abdominal response remarkably similar to the 7 year-old, which represented the swine corridors reasonably well (cf. Kent et al. 2009). Second, the relationship between thoracic stiffness and age does not appear to be monotonic over the entire lifespan, and existing scaling algorithms do not adequately describe the relationship. The two new subjects reported here follow the general trend reported in the 2009 study, with pediatric and elderly PMHS having similar thoracic stiffness under dynamic diagonal belt loading with a greater stiffness associated with the late adolescent and young adult years (Figure 5). Additional data are needed in the age range between 15 and 50 years.



Bolton, J. (2009) Viscoelastic response of the thorax under dynamic belt loading. *Traffic Injury Prevention* 10:1-8.

Thompson, E., Perkowski, P., Willarreal, D., Block, E., Brown, M., Wright, L., Akin, S. (2003) Morbidity and mortality of children following motor vehicle crashes. *Archives of Surgery* 138(2):142-145.

Tso, E, B Beaver and JA Halter (1993). Abdominal injuries in restraint pediatric passengers. *J Pediatric Surgery* 28(7): 915-919.

Trosseille, X., Chamouard, F., Tarriere, C. (1997) Abdominal injury risk to children and its prevention. *Proc. IRCOBI, Hannover, Germany*.

## APPENDIX – RAW DATA PLOTS

